IET Systems Biology

Research Article

IET Journals
The Institution of Engineering and Technology

Dynamics and robustness of the cardiac progenitor cell induced pluripotent stem cell network during cell phenotypes transition

ISSN 1751-8849
Received on 2nd November 2015
Revised on 1st April 2016
Accepted on 24th April 2016
doi: 10.1049/iet-syb.2015.0051
www.ietdl.org

Yuangen Yao[1], Chengzhang Ma[1], Haiyou Deng[1], Quan Liu[1], Wei Cao[1], Rong Gui[1], Tianquan Feng[2], Ming Yi[1] ✉

[1]*Department of Physics, College of Science, Huazhong Agricultural University, Wuhan, Hubei, People's Republic of China*
[2]*School of Teachers' Education, Nanjing Normal University, Nanjing, People's Republic of China*
✉ *E-mail: yiming@mail.hzau.edu.cn*

Abstract: Robustness is a fundamental characteristic of biological systems since all living systems need to adapt to internal or external perturbations, unpredictable environments, stochastic events and unreliable components, and so on. A long-term challenge in systems biology is to reveal the origin of robustness underlying molecular regulator network. In this study, a simple Boolean model is used to investigate the global dynamic properties and robustness of cardiac progenitor cell (CPC) induced pluripotent stem cell network that governs reprogramming and directed differentiation process. It is demonstrated that two major attractors correspond to source and target cell phenotypes, respectively, and two dominating attracting trajectories characterise the biological pathways between two major cell phenotypes. In particular, the experimentally observed transition between different cell phenotypes can be reproduced and explained theoretically. Furthermore, the robustness of major attractors and trajectories is largely maintained with respect to small perturbations to the network. Taken together, the CPC-induced pluripotent stem cell network is extremely robustly designed for their functions.

1 Introduction

Coronary heart disease has already been the leading cause of death in developed countries [1]. Recently, as a promising treatment option, stem-cell-based therapies have attracted considerable attention [2–4]. Especially, human-induced pluripotent stem cells (iPSCs) have emerged as an attractive donor cell source due to possessing the capacity of unlimited self-renewal and pluripotency [1, 5]. Self-renewal is the ability of embryonic stem cells (ESCs) to maintain the cell in a proliferative state for prolonged periods, while the pluripotency is the capability of ESCs to generate all cell types [6]. They are two defining property of ESCs. Human iPSCs share many similar features to human ESCs, although epigenetic characteristics are distinct in iPSCs [1]. As a reversed process of natural development, reprogramming can induce highly differentiated cells into iPSCs. The spermic work by Yamanaka and colleagues [5] showed that the overexpression of the pluripotency transcription factors (OCT4, SOX2, KLF4 and c-MYC) is sufficient to reprogramme somatic cells to iPSCs. It was later reported that iPSCs can be induced by viral integration of OCT4, SOX2 and KLF4, without c-MYC [7]. Furthermore, other combination of the pluripotency transcription factors (OCT4, SOX2, NANOG and LIN28) also can reprogramme somatic cells into iPSCs [8]. Among these transcription factors, OCT4, SOX2, KLF4 and NANOG are thought to be essential components of the core transcriptional circuitry for maintenance pluripotency and self-renewal [9, 10]. Recently, experimental studies have shown that cardiac progenitor cells (CPCs) were reprogrammed into iPSCs through lentiviral infection using OCT4, SOX2, KLF4 and c-MYC, and then established iPSCs derived from CPCs (CPC-iPSC) were differentiated into iPSC-derived cardiomyocytes (iPSC-CMs) [1]. The differentiation of iPSCs to cardiomyocytes (CMs) goes through the several distinct stages, including the generation of an early mesoderm, followed by a cardiac mesoderm specific to different established cardiovascular lineages [1]. In this experiment, MESP1 and ISL1 were chosen as markers for early cardiac mesoderm and cardiovascular progenitor cells, respectively [1]. MESP1 is a transcription factor indispensable for the specification of multipotent cardiovascular progenitors and the expression of cardiovascular transcription factors, while ISL1 is necessary for the formation of the right ventricle [1]. CPCs produce not only CMs but also other cell types observed in the normal heart [1]. From non-linear dynamic point of view, this phenomenon that CPCs are reprogrammed into iPSCs and further differentiated into iPSC-CMs is analogous to state transition between the different attractors in a non-linear dynamic system. The investigation of robustness properties of this multiple-attractors system from dynamic point of view will contribute to stem-cell-based medicine.

Biological systems are often subject to a variety of perturbations ranging from changing environment conditions to stochasticity in molecular processes [11, 12]. Therefore, biological systems require robustness, i.e. the capacity for sustained and precise function even in the moderate perturbation circumstances [13]. Such robustness has been widely observed over multiple scales of biological organisation, from the biochemical signalling pathway to the cellular level [13]. The study for the origin of robustness in biological systems from a network topological structure and dynamic process point of view is a hot area of research in systems biology [14]. A representative example proposed by Li *et al.* in 2004 [15] demonstrated robustness design in cell-cycle regulatory network of the budding yeast by a simple Boolean dynamical model. Later, Han and Wang [16] proposed energy landscape for the budding yeast cell cycle network to study the global robustness, and discovered a very robust funnelled potential landscape towards the global minimum, G1 state. In 2010, through the novel process-based approach, Wang *et al.* [17] decomposed the budding yeast cell cycle network into two sub-networks: minimal network which provides desired functionality and remaining network which confers robustness. Yang and co-workers [18] constructed mammalian G1/S transition regulatory (MGSTR) cancer network consisting of transcription factors, oncogenes, anti-oncogenes and microRNAs, and then investigated robustness properties of MGSTR by Boolean network theory. Although a number of efforts have been contributed to this area, these studies mainly focused on cell cycle network or cancer network. To our knowledge, few

robustness studies were implemented specifically for CPC-induced pluripotent stem cell network.

On the basis of the given network structure, the above-mentioned studies mainly focused on the robustness of network by using synchronous updating schemes of Boolean network. On the other hand, based on a given reliable trajectory in state space, a Boolean network was constructed to meet this function. Then, the robustness of the network was investigated under the noise and fluctuations in updating strategy [19]. The synchronous updating scheme is very attractive due to simplicity, but it is unable to deal with the variety of time scales in different types of biological processes. The asynchronous updating scheme, where the discrete states are updated in a heterogeneous way over time is a more realistic manner for modelling a given biological system. There are various different asynchronous updating methods, for example, in a random order, or in an order based on given properties. However, the different asynchronous updating schemes may cause different dynamic behaviours. On the basis of hormone abscisic acid signal transduction network in plant, the dynamic behaviours were systematically investigated by using one synchronous and three asynchronous updating methods [20]. More realistically, the probabilistic Boolean network should be incorporated to take into account the factors, e.g. the uncertainty in the data and the model selection, relative influence and sensitivity of genes, and so on [21].

Recent experimental researches in cell reprogramming have shown the possibility of transition between different cell phenotypes [1, 5, 22, 23], which triggered a fascinating theoretical question about quantifying the transition process from one type of cell into another. Therefore, many efforts have been made to define the quasi-potential landscape which can map cell's gene regulatory network into its phenotypic states and dynamic behaviours in a formally accurate fashion yet intuitively plausible [24–27]. These studies used equation-based approaches to model cell process by integrating molecular biology details piece-by-piece. These equation-based approaches have typically many parameters, thus need sufficient experimental data to determine all these parameters. Recently, by simplifying the high-dimensional landscape to a batch of discrete states and transition paths among them, a novel equation-based methodology was proposed to describe this cell phenotypic transition [28], and relieved difficulties in parameter determination. Furthermore, this approach can reproduce some observed phenomena or behaviours, and manifest quantitatively predictive power [28]. However, the robustness properties of epigenetic state network were not investigated particularly in their research.

In this work, Boolean network theory was used to investigate the global dynamics process and robustness properties of CPC-induced pluripotent stem cell network based on the coarse-graining epigenetic state network provided by Wang *et al.* [28]. It was found that, two biggest attractors characterise the source and target cell phenotypes, respectively. Furthermore, the trajectories between them just correspond to the biological pathways of cell reprogramming and directed differentiation, respectively. Meanwhile, intermediate states are predicted. Through network perturbation approach, it was shown that, CPC-induced pluripotent stem cell network is still robustly constructed even during cell phenotypic transition.

2 Model and results

2.1 Boolean model of CPC-iPSC-CMs network

It was reported that CPCs were reprogrammed into iPSCs and further differentiated into iPSC-CMs [1]. For these studies of reprogramming somatic cells to iPSCs, OCT4, SOX2, KLF4 and NANOG are often used as pluripotency transcription factors to induce reprogramming, which are thought to be essential components of the core transcriptional circuitry for maintenance pluripotency and self-renewal [9, 10]. The induction and specification of cardiac mesoderm are the critical differentiation processes from iPSCs to CMs [1, 29], which were marked by using MESP1 and ISL1 in the above-mentioned experiment, respectively [1]. Here, focusing on the key pluripotency transcription factors of the core transcriptional circuitry for maintenance pluripotency and self-renewal, as well as markers of critical differentiation processes, a high coarse-graining network was constructed based on the work of Wang *et al.* [28] to capture key features of CPC-iPSC-CMs system, which comprised 9 nodes and 37 edges (Fig. 1). Then, global dynamic process and robustness properties of CPC-iPSC-CMs system was investigated by using Boolean network theory.

In principle, the time scales of interaction are very different in the network. Therefore, dynamic model would include various rate parameters and time delay. Additionally, the change of molecular concentration is continuous rather than two (high or low) discrete states. However, expression profiles of most network components in CPC-iPSC-CMs system are switch-like [1]. More importantly, only higher-level network properties involving the global dynamics and robustness were investigated in this study. As previously described, the expression of components was simplified into a total-or-nothing process. Then, 1 and 0 states were used to characterise active and inactive state of network components, respectively [15, 17, 18]. Taken together, a Boolean model was applied to simulate the dynamic behaviours of CPC-iPSC-CMs system. In the Boolean model, the network state in the next time step is determined by current network state through a synchronous updating rule presented below [15]

$$S_i(t+1) = \begin{cases} 1, & \sum_j a_{ji} S_j(t) > 0 \\ 0, & \sum_j a_{ji} S_j(t) < 0 \\ S_i(t), & \sum_j a_{ji} S_j(t) = 0 \end{cases} \quad (1)$$

where $S_i(t)$ stands for the state of the ith node at time t. Moreover, (a_{ji}) is the $N \times N$ matrix determining the network structure. Here, $a_{ji} = 1$, 0 or $-r$ denote, respectively, the activation, no interaction or repression of node j to node i (Table 1). The relative dominance of repression over stimulation is characterised by the parameter r. Repression occupies a dominant position over stimulations for most biomolecular interactions [17]. Moreover, the network dynamics, which is usually not sensitive to the value of r, is mainly dominated by network topology [17]. Therefore, r was assigned as 10,000 ($\geq$1) during simulation (Table 1).

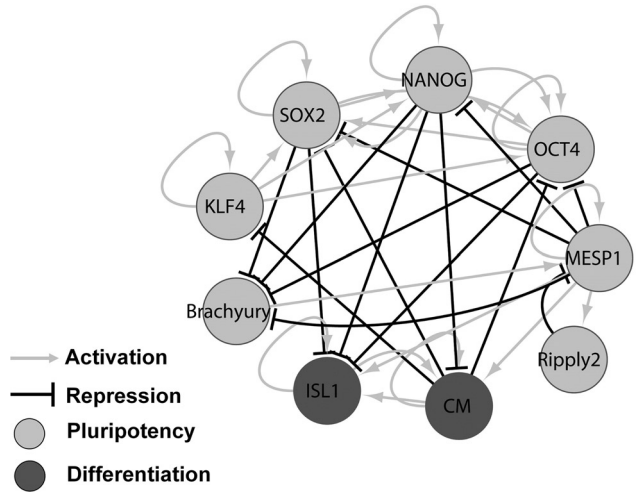

Fig. 1 *Topology of CPC-induced pluripotent stem cell network. Each node denotes transcription factor involved in cell reprogramming and directed differentiation. The grey arrow indicates activation and the black arrow represents repression. Gene markers coloured in light grey are found in cells being in pluripotent states, while those coloured in dark grey are found for differentiated state phenotypes*

Table 1 Structure parameter a_{ji} of CPC-induced pluripotent stem cell network. $a_{ji} = 1$, 0, or $-r$ denote, respectively, the activation, no interaction or repression of node j to node i

	NANOG	OCT4	SOX2	KLF4	Brachyury	MESP1	Ripply2	ISL1	CM
NANOG	1	1	1	1	0	$-r$	0	0	0
OCT4	1	1	1	1	0	$-r$	0	0	$-r$
SOX2	1	1	1	1	0	$-r$	0	0	$-r$
KLF4	0	0	0	1	0	0	0	0	$-r$
Brachyury	$-r$	$-r$	$-r$	0	0	$-r$	0	0	0
MESP1	0	0	0	0	1	1	$-r$	0	0
Ripply2	0	0	0	0	0	1	0	0	0
ISL1	$-r$	$-r$	$-r$	0	0	1	0	1	1
CM	$-r$	0	0	0	0	1	0	1	1

2.2 Dynamic properties of CPC-iPSC-CMs network

The network state is the vector of 0 or 1, i.e. node's value. Totally, 9-node network has $2^9 = 512$ states in the state space. From a given start state, by iteratively applying the updating rule of (1), a well-defined sequence or trajectory of network states occurs and ends up in a stable state called an attractor. The number of states that converge to an attractor is defined as size of basin. Starting from each one of the 512 possible states, we can enumerate all possible attractors and trajectories for the CPC-iPSC-CMs network.

It was found that the system dynamics gives rise to ten different attractors (Fig. 2). Most of the network states flow into two biggest stationary state attractors, which account for 41.99 and 27.34% in 512 states, respectively (Fig. 2). The previous study by Wang *et al.* examined the published microarray data to estimate the expression level of corresponding regulators, and then defined the major states/phenotypes for cell phenotypic transitions (see details in Table S5 in Wang's literature) [28]. According to the original results from Wang *et al.* (see details in Table S5 in Wang's literature) [28], a heatmap was redrawn to describe the major states/phenotypes and the expression level of corresponding regulators (Fig. 2*a*). As shown in Fig. 2, the first largest attractor 'state(7)' corresponds to target cell phenotype, where cells are being in differentiated states (Fig. 2*b*); the second largest attractor 'state(452)' corresponds to source cell phenotype, where cells are being in pluripotent states (Fig. 2*c*). Furthermore, except Ripply2 being high expression in our results yet low expression in Wang's results, the second largest attractor in our results perfectly matches the predicted cell state of iPSCs reported in Wang *et al.* [28]. (Fig. 2*c*; see details in Fig. 5*a* and Table S5 in Wang's literature). CM, ISL1 and Ripply2 are the markers of CMs, cardiac progenitor and mesoderm, respectively [28]. They are high expression in our predicted cell state corresponding to the first largest attractor (Fig. 2*b*), while only CM was expressed in a high level in Wang's results for the terminal phenotype. Although the cell phenotype corresponding to the first largest attractor in our results did not exactly match the predicted cell state of CMs in Wang's results (Fig. 2*b*; see details in Fig. 5*a* and Table S5 in Wang's literature), high expression of CM, ISL1 and Ripply2 suggested that cells are being in differentiated states, i.e. target cell phenotype (Fig. 2*b*). Then, Cytoscape was used for visual representation of the system dynamics in the state space [30]. Each node indicates a network state of the system, and arrows between states represent the direction of dynamic flow from one state to another (Fig. 3). We can see that the network states flow into some major attractors corresponding to cell phenotypes of CPC-iPSC-CMs network, and the dynamic flow of network states is convergent into some dominant attracting trajectories corresponding to biological pathways (Fig. 3). It was illustrated that two major attractors in the CPC-iPSC-CMs network correspond to target and source cell phenotypes (Figs. 2*b* and *c*), respectively, and two dominating trajectories describe the transition pathways between two major cell phenotypes (Figs. 4*b* and *c*). During differentiation into CMs, the expression levels of pluripotent stem cell markers, NANOG, OCT4 and SOX2 were significantly down-regulated (Fig. 4*b*). However, the expression levels of ISL1 and CM were significantly up-regulated in differentiated cells (Fig. 4*b*). Furthermore, the observation in the trajectory matches with the fact that CMs are derivatives of the mesoderm germ during mammalian development (Fig. 4*b*). Thus, this biological pathway stands actually for directed differentiation from iPSCs to CMs (Fig. 4*b*). Starting from the biggest node, the pluripotency appears decreasing at first and then increasing gradually in the clockwise direction (Fig. 4*c*), whereas the differentiation degree of cells appears increasing at first and then decreasing gradually (Fig. 4*c*). Therefore, this pathway denotes cyclic process involving cell reprogramming and directed differentiation (Fig. 4*c*). The plausibility for a cell's stationary state to be a big attractor of network is to guarantee the stability of cell state. Under normal conditions, the cell stays at stationary attractor until receives the signal for another transition.

2.3 Robustness of major attractors

To investigate how likely a big attractor can arise by chance, 1000 random networks with the same numbers of nodes and edges in each colour as the CPC-iPSC-CMs network were constructed and analysed. It was found that the distribution of basin size of attraction follows a power-law (Fig. 5*a*). Only 11.41 and 18.95% attractors are equal to or larger than the first and second attractors, respectively.

The relative change in the basin size (B) for major attractors, $\Delta B/B$ can be used to measure robustness of network in the presence of perturbation. To calculate this value, as previously described, CPC-iPSC-CMs network were perturbed by deleting an edge, adding a grey or black edge between nodes that are not linked by an edge, or switch a black edge to grey and vice versa [15]. Totally, there are 243 perturbations composing of 37 perturbations by deleting edges, 132 perturbations by adding edges and 74 perturbations by switching edges. Each kind of perturbation produces a collection of random networks. Therefore, given an attractor, the distributions of $\Delta B/B$ for this attractor were obtained and plotted (Figs. 5*b–d*). It was shown that only a very small proportion of perturbations can completely remove the given attractor. The relative changes of the basin size are small for most of perturbations (Figs. 5*b–d*). To investigate whether the robustness remains against perturbations of deleting a node, the two largest attractors were analysed for nine perturbations. The source and target cell phenotypes remain robust against most perturbations of deleting node, e.g. OCT4, SOX2, KLF4, Brachyury and Ripply2 (Fig. S1). The original network provided by Wang *et al.* was regained by adding FB into our network (Fig. S2A), which was used to describe the fibroblast (Fib)-induced pluripotent stem cell-CMs (Fib-iPSC-CMs) system [28]. In this system Fibs can be induced to CMs directly or through iPSCs indirectly [28]. Starting from each one of the $2^{10} = 1024$ possible states, we can enumerate all possible attractors for expanded network. For this expanded network, the first and second largest attractors correspond to phenotypes of cells in differentiated and pluripotent states, respectively (Fig. S2B-D). Note that the expanded network can produce exactly the same attractors in the pluripotent state with that of our network (Fig. S2D). FB, ISL1 and CM are markers of Fib, cardiovascular progenitor, and CM, respectively [28]. The high expression of FB, CM and ISL1 not only suggested that direct and indirect pathways coexist for Fib-iPSC-CMs, but also implied that our network is robust when

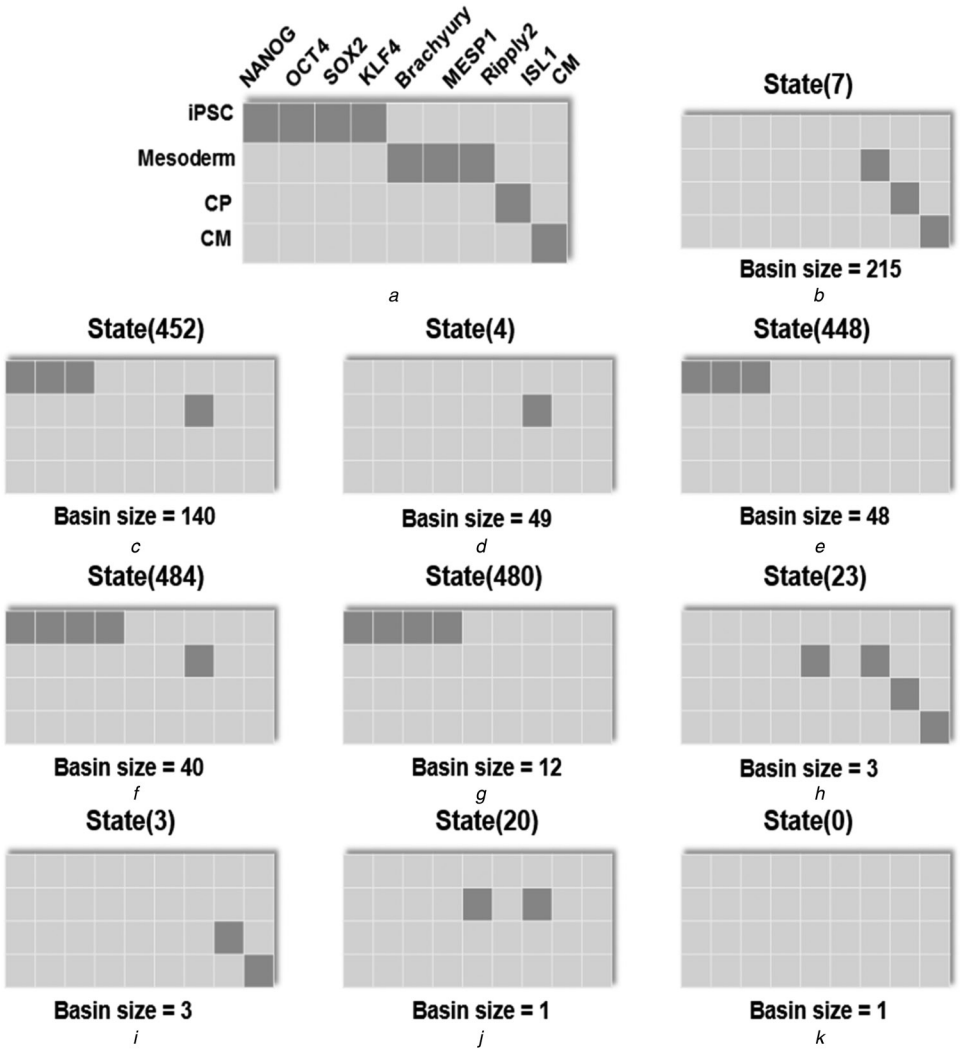

Fig. 2 *Basin size and state of attractors. Attractor is represented as 'state(x)', where x is decimal number, and obtained by transforming the binary network state*

a Definition of major states/phenotypes and their expression level in previous study [28]
b Attractor of 'state(7)'
c Attractor of 'state(452)'
d Attractor of 'state(4)'
e Attractor of 'state(448)'
f Attractor of 'state(484)'
g Attractor of 'state(480)'
h Attractor of 'state(23)'
i Attractor of 'state(3)'
j Attractor of 'state(20)'
k Attractor of 'state(0)'

adding FB. To investigate the effect of relative dominance of repression, i.e. r on the robustness of major attractors, the basin size of two main attractors were obtained under various parameter of r. The cases $r \geq 5$ produce exactly the same results and are only slightly different from the cases $r = 2$–4 (Fig. S3A). This suggested that the major attractors are robust under the parameter perturbation of r. For the case $r = 1$, there are no dominant attractors among 33 attractors, and the specified attractors of 'state (7)' and 'state(452)' are no longer major attractors (Fig. S3B). Therefore, the function of the network was destroyed. Taken together, there are two major attractors in CPC-iPSC-CMs network, and they are relatively robust even in the presence of various fluctuations.

2.4 Robustness of major trajectories

To investigate the effects of these perturbations on major trajectories, i.e. the biological pathway itself, the robustness of major trajectories were analysed. Some above-mentioned perturbations alter the basin size of major attractors significantly, thereby, ultimately destroy system function. To satisfy some basic biological functions of CPC-iPSC-CMs network, only 171 perturbations were kept for further analysis of trajectory's robustness. Since they can guarantee some basic biological constraints: at least two biggest attractors corresponding to the source and target cell phenotypes, respectively. Then, the occurrence of dynamic flow arrows (or edges) in the collection of random networks produced by 171 perturbations was drawn. Remarkably, we observed that the occurrences of edges in the state space jump abruptly between 124 and 14 (Fig. 6). It means that only a small fraction of dynamic flow arrows (18.84%) is used to maintain the functions of CPC-iPSC-CMs network, while the other likely arise by cell-to-cell non-genetic variations due to extrinsic and intrinsic noises. After removing the edges with low occurrence ($\leq$14), we can reproduce two major trajectories which are identical to ones without any perturbation (Fig. 3 and Fig. S4). When altering the value of r, for two major trajectories, the cases $r \geq 4$ produce

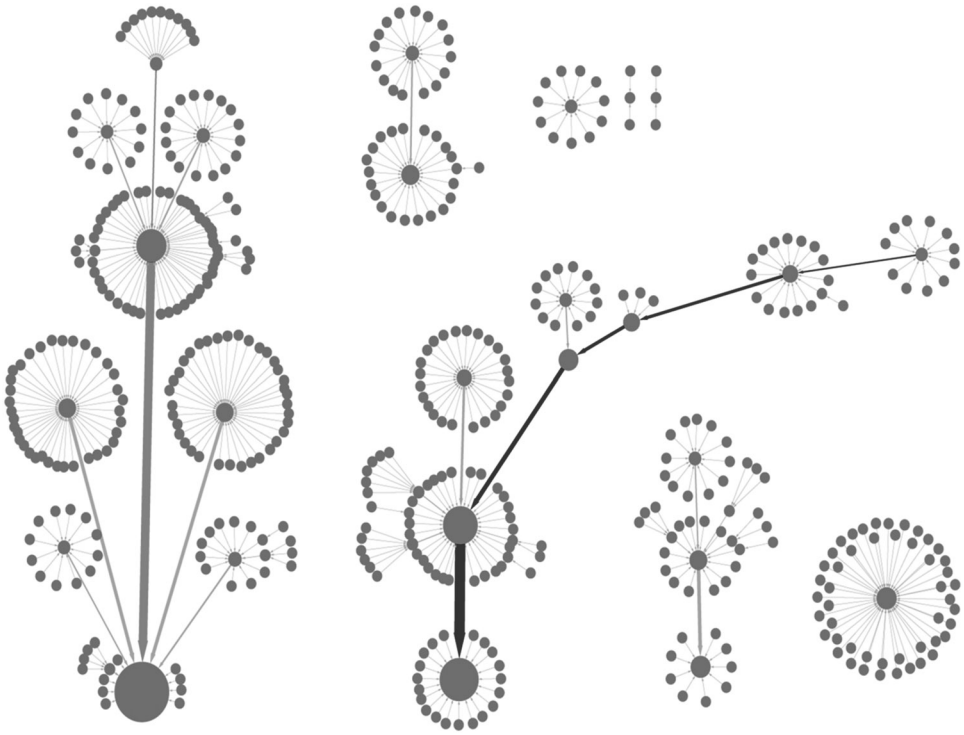

Fig. 3 *Dynamic trajectories of CPC-induced pluripotent stem cell network in state space. Every state converges towards a specific stable attractor. Each node represents one specific network state. Two largest nodes correspond to the target and source cell phenotypes, respectively. Arrows between states stand for the flow direction from one state to another. The thickness of arrow and edge reflect strength of attraction, i.e. the number of states passing through them. The trajectory coloured in light grey corresponds to directed differentiation process, while the trajectory coloured in dark grey is used for cyclic process composing of cell reprogramming and directed differentiation*

exactly the same results and are distinct different from the cases $r = 2$ or 3 (Fig. S5). It was suggested, the major trajectories are robust under the parameter perturbation of r. The above analysis showed that major trajectories are also relatively robust in the presence of perturbation. Taken together, the CPC-iPSC-CMs network is robustly designed for their functions.

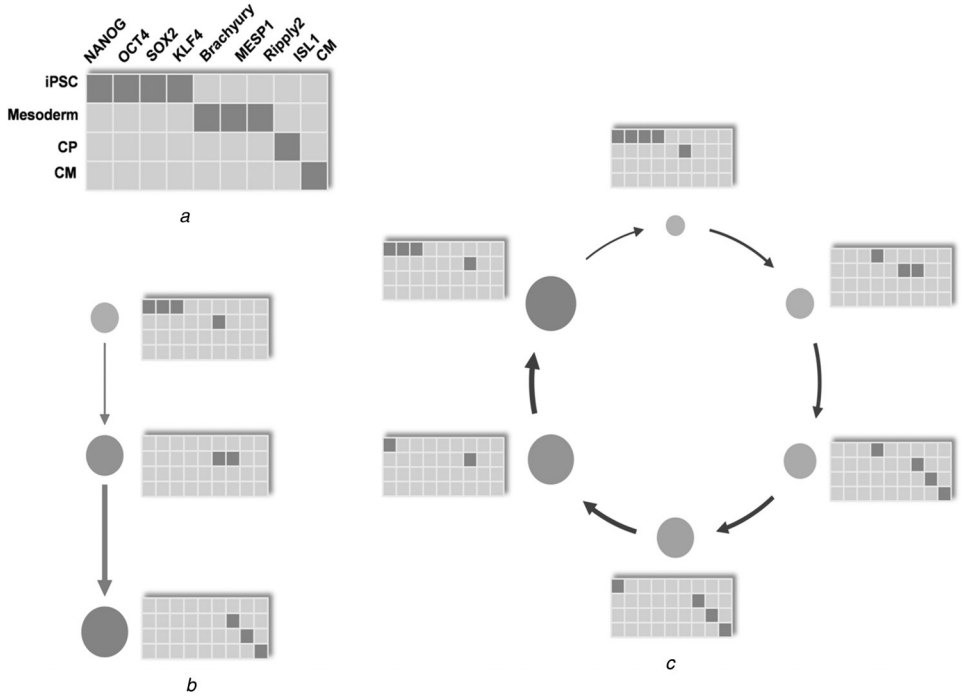

Fig. 4 *Gene markers for major states/phenotypes and their expression level during the different processes*

a Definition of major states/phenotypes and their expression level in previous study [28]. Dark grey and light grey indicate high and low expression, respectively
b Dynamic trajectories and gene markers' expression level during directed differentiation process. The size of node and edges represents strength of attraction, i.e. the number of states passing through them. Change in deepness of colour is a metaphorical representation of time-dependent dynamic process
c Dynamic trajectories and gene markers' expression level during cyclic process involving cell reprogramming and directed differentiation

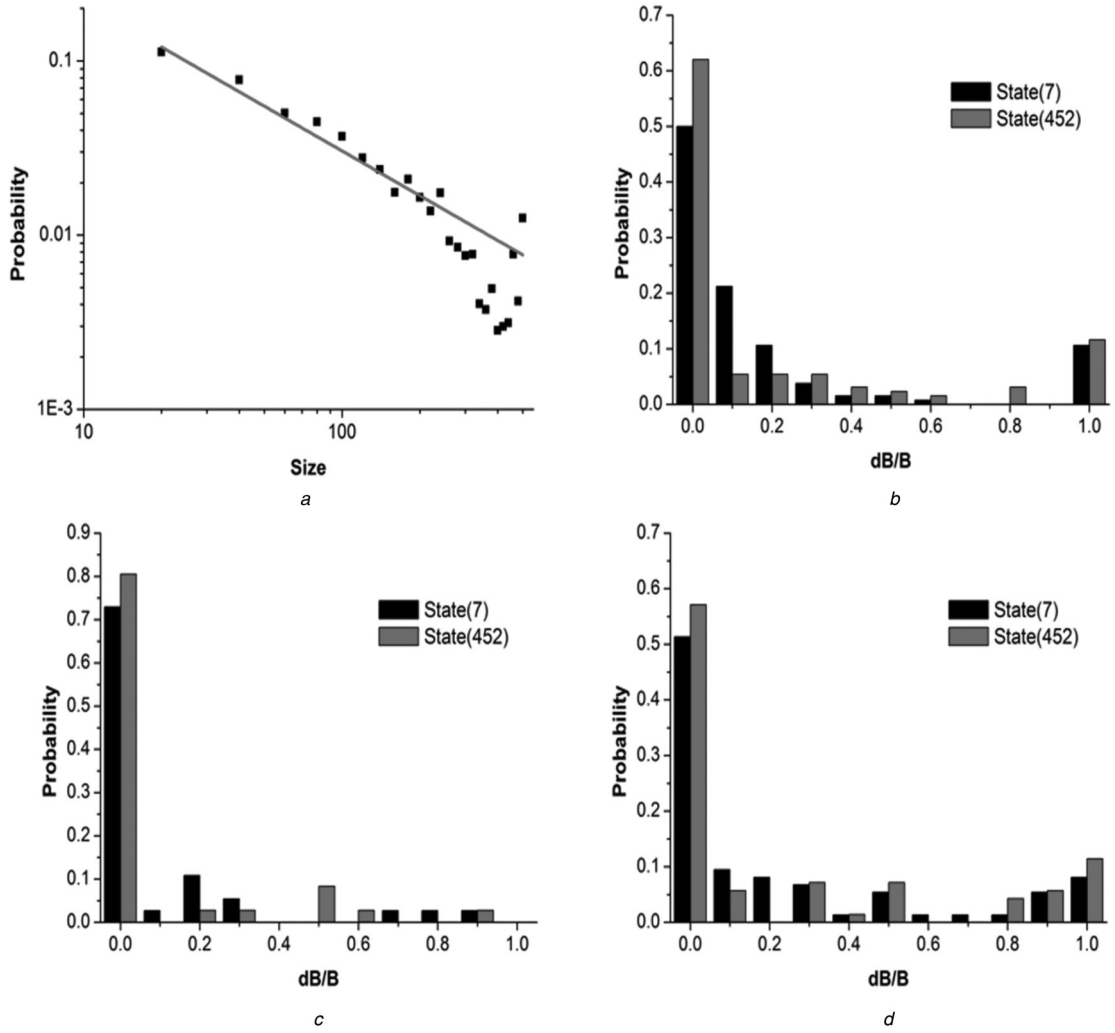

Fig. 5 *Robustness test of two biggest attractors through network perturbation approach*

a Attractor size distribution of random networks
b Histogram of the relative changes of the basin size for two biggest attractors through adding 132 edges
c Deleting 37 edges
d Switching 74 edges

3 Discussion

Modelling the molecular regulator network that governs cell reprogramming and directed differentiation process is a long-term challenge in systems biology. Although the CPC-iPSC-CMs network is a very coarse-graining, based on the Boolean dynamical theory, it provides a description of cell phenotypic transition in a formally accurate fashion yet intuitively plausible. From structural and dynamic point of view, our analysis has yielded significant insights into the global dynamics and robustness of CPC-iPSC-CMs network. The biological cell phenotypes during reprogramming and directed differentiation just correspond to two biggest attractors, respectively. Moreover, the biological transition pathways among source and target cell phenotypes are two major attracting trajectories. Even when the network is perturbed, these properties are largely preserved. These results demonstrate that CPC-iPSC-CMs network is extremely robustly designed for their functions.

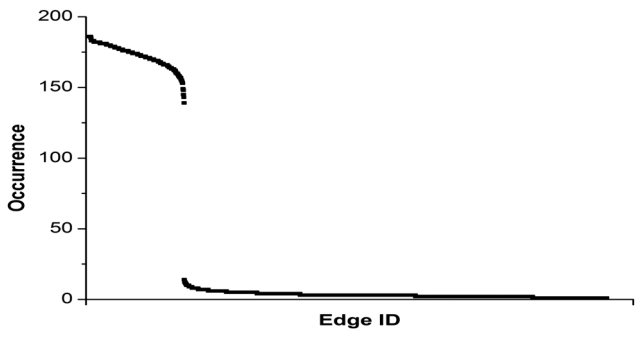

Fig. 6 *Distribution of occurrence of dynamic flow arrows. An abrupt jump of occurrences of edges is shown between 124 and 14*

The approach we present in this work is reasonable. However, it should be pointed out that some limitations are originated from two basic simplifications: highly coarse-graining and Boolean model. The coarse-graining procedure simplifies theoretical study in favour of revealing the underlying mechanism, but loses much information about system. Moreover, Boolean model roughly maps molecular concentrations into two molecular states: active or inactive. In the Boolean model, the interactions between the molecules are either activate or repressive, and these biochemical reactions are in the same time scales. However, such assumptions are standard for Boolean theory.

Differential equation-based approaches are established by integrating molecular biology details piece-by-piece. They have typically many parameters, thus need sufficient experimental data to determine all these parameters. In addition, they are subjected to innate shortcomings, such as, the difficulty in parameter optimisation, the sensibility of parameter and initial value, and so

on. Boolean model is typically used in place of differential equation-based approaches to elicit higher-level network properties. Simple though it is, it captures how the topology constrains the dynamics of the molecular expression levels, and demonstrates that CPC-iPSC-CMs network is extremely robustly designed for their functions.

Our results not only theoretically explain the possibility of transition between different cell phenotypes, but also suggest the possibility of optimising the transition process. The optimal pathways are the easiest pathway for transition from one phenotype to another. Intuitively, the transition is more efficient if external perturbations exist. Since some perturbations reduce 'barrier height' between attractors or drive the system away from attracting basins, it makes system easy to relax to various different basins, and then results in the change of cell phenotypes. Additionally, the trajectories involve a collection of intermediate states, which suggests that these externally perturbations are time-dependent. However, in practice, more qualitative and quantitative information about structure and dynamics of CPC-iPSC-CMs network are required to optimise the transition process.

4 Acknowledgments

The authors thank Dr. Ya Jia (CCNU), Dr. Lijian Yang (CCNU), Dr. Anbang Li (CCNU) and Dr. Zhan Xuan (CCNU) for their helpful suggestions on the project implementation. This work was supported by the Fundamental Research Funds for the Central Universities (grant nos. 2662014BQ069 and 2662015QC041), the National Natural Science Foundation of China (grant nos. 11275259 and 91330113) and Huazhong Agricultural University Scientific & Technological Self-innovation Foundation (Program No. 2015RC021).

5 References

1 Sanchez-Freire, V., Lee, A.S., Hu, S., *et al.*: 'Effect of human donor cell source on differentiation and function of cardiac induced pluripotent stem cells', *J. Am. Coll. Cardiol.*, 2014, **64**, (5), pp. 436–448
2 Srivastava, D., Ivey, K.N.: 'Potential of stem-cell-based therapies for heart disease', *Nature*, 2006, **441**, (7097), pp. 1097–1099
3 Young, P.P., Schafer, R.: 'Cell-based therapies for cardiac disease: a cellular therapist's perspective', *Transfusion*, 2014, **55**, (2), pp. 441–451
4 Matsa, E., Burridge, P.W., Wu, J.C.: 'Human stem cells for modeling heart disease and for drug discovery', *Sci. Transl. Med.*, 2014, **6**, (239), p. 239ps236
5 Takahashi, K., Tanabe, K., Ohnuki, M., *et al.*: 'Induction of pluripotent stem cells from adult human fibroblasts by defined factors', *Cell*, 2007, **131**, (5), pp. 861–872
6 Zhang, P., Andrianakos, R., Yang, Y., *et al.*: 'Kruppel-like factor 4 (Klf4) prevents embryonic stem (Es) cell differentiation by regulating Nanog gene expression', *J. Biol. Chem.*, 2010, **285**, (12), pp. 9180–9189
7 Aoi, T., Yae, K., Nakagawa, M., *et al.*: 'Generation of pluripotent stem cells from adult mouse liver and stomach cells', *Science*, 2008, **321**, (5889), pp. 699–702
8 Yu, J., Vodyanik, M.A., Smuga-Otto, K., *et al.*: 'Induced pluripotent stem cell lines derived from human somatic cells', *Science*, 2007, **318**, (5858), pp. 1917–1920
9 Boyer, L.A., Lee, T.I., Cole, M.F., *et al.*: 'Core transcriptional regulatory circuitry in human embryonic stem cells', *Cell*, 2005, **122**, (6), pp. 947–956
10 Brouwer, M., Zhou, H., Nadif Kasri, N.: 'Choices for induction of pluripotency: recent developments in human induced pluripotent stem cell reprogramming strategies', *Stem Cell Rev.*, 2016, **12**, (1), pp. 54–72
11 Bluthgen, N., Legewie, S.: 'Robustness of signal transduction pathways', *Cell. Mol. Life Sci.*, 2013, **70**, (13), pp. 2259–2269
12 Kitano, H.: 'Biological robustness', *Nat. Rev. Genet.*, 2004, **5**, (11), pp. 826–837
13 Shinar, G., Feinberg, M.: 'Structural sources of robustness in biochemical reaction networks', *Science*, 2010, **327**, (5971), pp. 1389–1391
14 Kitano, H.: 'Towards a theory of biological robustness', *Mol. Syst. Biol.*, 2007, **3**, pp. 137–130
15 Li, F., Long, T., Lu, Y., *et al.*: 'The yeast cell-cycle network is robustly designed', *Proc. Natl. Acad. Sci. USA*, 2004, **101**, (14), pp. 4781–4786
16 Han, B., Wang, J.: 'Quantifying robustness and dissipation cost of yeast cell cycle network: the funneled energy landscape perspectives', *Biophys. J.*, 2007, **92**, (11), pp. 3755–3763
17 Wang, G., Du, C., Chen, H., *et al.*: 'Process-based network decomposition reveals backbone motif structure', *Proc. Natl. Acad. Sci. USA*, 2010, **107**, (23), pp. 10478–10483
18 Yang, L., Meng, Y., Bao, C., *et al.*: 'Robustness and backbone motif of a cancer network regulated by Mir-17–92 cluster during the G1/S transition', *PLoS One*, 2013, **8**, (3), p. e57009
19 Schmal, C., Peixoto, T.P., Drossel, B.: 'Boolean networks with robust and reliable trajectories', *New J. Phys.*, 2010, **12**, (11), p. 113054
20 Saadatpour, A., Albert, I., Albert, R.: 'Attractor analysis of asynchronous Boolean models of signal transduction networks', *J. Theor. Biol.*, 2010, **266**, (4), pp. 641–656
21 Shmulevich, I., Dougherty, E.R., Kim, S., *et al.*: 'Probabilistic Boolean networks: a rule-based uncertainty model for gene regulatory networks', *Bioinformatics*, 2002, **18**, (2), pp. 261–274
22 Zhang, J., Wilson, G.F., Soerens, A.G., *et al.*: 'Functional cardiomyocytes derived from human induced pluripotent stem cells', *Circ. Res.*, 2009, **104**, (4), pp. e30–e41
23 Efe, J.A., Hilcove, S., Kim, J., *et al.*: 'Conversion of mouse fibroblasts into cardiomyocytes using a direct reprogramming strategy', *Nat. Cell Biol.*, 2011, **13**, (3), pp. 215–222
24 Wang, J., Li, C., Wang, E.: 'Potential and flux landscapes quantify the stability and robustness of budding yeast cell cycle network', *Proc. Natl. Acad. Sci. USA*, 2010, **107**, (18), pp. 8195–8200
25 Zhou, J.X., Huang, S.: 'Understanding gene circuits at cell-fate branch points for rational cell reprogramming', *Trends Genet.*, 2011, **27**, (2), pp. 55–62
26 Li, C., Wang, J.: 'Quantifying cell fate decisions for differentiation and reprogramming of a human stem cell network: landscape and biological paths', *PLoS Comput. Biol.*, 2013, **9**, (8), p. e1003165
27 Li, C., Wang, J.: 'Quantifying Waddington landscapes and paths of non-adiabatic cell fate decisions for differentiation, reprogramming and transdifferentiation', *J. R. Soc. Interface*, 2013, **10**, (89), p. 20130787
28 Wang, P., Song, C., Zhang, H., *et al.*: 'Epigenetic state network approach for describing cell phenotypic transitions', *Interface Focus*, 2014, **4**, (3), p. 20130068
29 Yang, L., Soonpaa, M.H., Adler, E.D., *et al.*: 'Human cardiovascular progenitor cells develop from a Kdr+ embryonic-stem-cell-derived population', *Nature*, 2008, **453**, (7194), pp. 524–528
30 Cline, M.S., Smoot, M., Cerami, E., *et al.*: 'Integration of biological networks and gene expression data using cytoscape', *Nat. Protoc.*, 2007, **2**, (10), pp. 2366–2382